ELSEVIER

Mathematical Biosciences 165 (2000) 115–134

Mathematical Biosciences

www.elsevier.com/locate/mbs

Early HIV infection in vivo: branching-process model for studying timing of immune responses and drug therapy

David Wick *, Steven G. Self

Fred Hutchinson Cancer Research Center, MW-500, P.O. Box 19024, 1100 Fairview Avenue N, Seattle, WA 98109-1024, USA

Received 14 July 1999; received in revised form 9 March 2000; accepted 30 March 2000

Abstract

We propose a stochastic, branching-process model of early events in vivo in human or simian immunodeficiency virus (HIV or SIV) infection and study the influence that the time of appearance of virus-specific antibodies or cytotoxic cells, or of administration of antiretroviral drugs, has on the probability of progression to a chronic infection. In some biological scenarios, our model predicts that a few days' delay in response or intervention would make little difference, while in others it would be highly deleterious. We show that prophylactic efficacy does not require perfect efficiency at neutralizing infectious virus. Data from a trial of PMPA, a potent antiretroviral drug, as post-exposure therapy for SIV infection in macaques, reported by C.-C. Tsai, P. Emau, K.E. Follis, T.W. Beck, R.E. Beneveniste, N. Bischofberger, J.D. Lifson, W.R. Morton (J. Virol. 72 (1998) 4265), provides a test of the model. We show that their observations are consistent with a branching-process without invoking supplementary viral- or host-variability. Finally, most animal trials of antiviral drugs or vaccines use very high viral inoculums; our model demonstrates that in such experiments we risk greatly underestimating the efficacy of these agents.

Keywords: Primary HIV infection; Primary SIV infection; Early intervention; Antiretroviral treatment; In vivo kinetics; PMPA; Pathogen eradication; HAART; Branching-process models; Extinction

1. Introduction

The primary target of the human immunodeficiency virus (HIV) is the T-lymphocyte bearing the CD4 molecule on its surface – although, in sexual transmission, the first cellular victim may be a monocyte-derived macrophage or dendritic cell (DC), quite plausibly a skin-resident DC called

* Corresponding author. Tel.: +1-206 667 7908; fax: +1-206 667 4812.
E-mail addresses: wick@hivnet.fhcrc.org (D. Wick), sgs@hivnet.fhcrc.org (S.G. Self).

0025-5564/00/$ - see front matter
PII: S0025-5564(00)00013-4

a Langerhans cell (LC) [1]. But, whatever the lineage of this 'index' cell, its migration to a T-cell-rich zone of a lymph node founds the in vivo 'epidemic'. Soon infected-cell counts explode into the billions, while newly budded virions spill into peripheral blood, seeding the infection into multiple tissue compartments [2,3]. After a few weeks, the viral load subsides by several orders-of-magnitude [4] for reasons that are still controversial but presumably involve an immune response [5,6], a target-cell limitation [7,8], or both.

We are interested in the earliest physiological events in HIV infection and in the immune response or drug intervention required to block progression to a chronic infection. HIV is not easily acquired – for sexual transmission, estimates from partner studies place the risk to the uninfected partner at one percent or less per unprotected sex act, [9,10]. Creating that first productively-infected cell might be the principal bottleneck, with progression afterward a near certainty. Alternatively, a number of cells might be infected initially, but the chance that any go on to establish an infection-chain might be small. In either case, the ability to further lower the odds that the infection spreads beyond these 'founder' cells might define efficacy in a vaccine or drug against primary HIV. (That merely lowering the infection 'set-point' could represent a kind of efficacy we discuss briefly in the last section.)

Clearly, the timing of early in vivo events – so difficult to observe directly – matters. Perhaps HIV-specific antibodies and cytotoxic T-lymphocytes (CTLs) appear too late, like smokejumpers arriving after flames have leapt to branches and crowns. If so, how should we weight rapidity, relative to potency, of the immune response when assessing vaccines? Of more immediate clinical interest, how quickly must patients begin antiretroviral therapy after exposure? Would a week's delay matter? And for how long must treatment be continued?

Another interesting question concerns the role of chance in drug and vaccine trials. In the next-to-last section, we consider a recent trial of an antiretroviral drug, a nucleoside analogue called PMPA, as post-exposure prophylaxis against simian immunodeficiency virus (SIV) infection in macaques [11]. The outcomes – viral eradication or treatment failure – varied both with time post-exposure before initiating therapy and time-on-therapy. We show that the pattern of outcomes can be explained purely by stochastic events in the infection branching-process, without assuming variable pathogen- or host-factors.

The infectious dose used in animal trials is also of interest. Investigators typically administer 5–100 times the dose at which 50% of the animals become infected (the so-called 50%-animal-infectious-dose, or AID50), to limit trial expenses. But use of such large inoculums, relative to doses likely in sexual transmission, biases the test against less-than-perfect but still potentially valuable drugs or vaccines. In Section 6, we ask what might have happened in the PMPA trial if smaller inoculums were used. We conclude that, at the higher inocula, we might dismiss a therapeutically-useful drug.

Now to model choice. Ordinary differential equations (ODEs) have been used for nearly a decade to explore AIDS pathogenesis, [12,13], and have even been applied to PMPA treatment of primary disease, [14]. Although rate equations are appropriate when numbers grow large and mass-action laws dominate, they cannot describe fluctuations or extinctions. Occasionally, ODE modelers supplement their deterministic equations with 'noise' terms, turning them into stochastic differential equations (SDEs) [15]. Extinction becomes possible; unfortunately, it occurs in small populations where all 'macroscopic' approximations break down.

Nineteenth century demographers studying extinction of bourgeois family names first introduced branching processe [16]. In the twentieth century, population biologists applied branching

models to diffusion of a genetic trait, and mathematical epidemiologists to cancer. In carcinogenesis, transformed cells give rise to clones which either grow to establish a tumor or go 'extinct', [17,18]. The obvious analogy to eradicating HIV was first noted in [13].

The two pictures – deterministic and stochastic – suggest somewhat different intervention strategies. In ODEs, the 'basic reproductive number', usually written R_0, must exceed unity for an infection to spread [19]. If so, the infection cannot die out – according to the model. ODE modelers usually propose interventions driving R_0 below one, [14]. Branching-process models have a similar quantity with a similar interpretation – the expected number of secondary infections caused by the primary infection in its lifetime. But to avoid confusion, we write it as R_b (b for branching). Processes with $R_b > 1$ are called 'super-critical' in the probability literature [16]. Although a super-critical process grows *on average*, nevertheless the extinction probability – which we denote by 'QI' (E and P being unavailable in a probabilistic context) – is not zero. Indeed, if R_b decreases towards one, QI approaches one. Thus, in branching-process models decrementing the reproduction parameter can confer a benefit, even without completely suppressing growth.

The models we develop for early HIV infection lie in the general class of 'multi-type, age-dependent' branching processes [20], but have certain novel features. We relegate the mathematical details to later sections and an appendix, and discuss the biological assumptions next.

2. Biological assumptions

First, the inevitable acronyms. We refer to all cells of monocyte lineage, including DCs and LCs, collectively as 'M's; once infected they become 'PIM's, short for 'productively-infected, monocyte-derived cells'. Similarly, 'Ts' are T-cells and a 'PIT' a productively-infected T-cell. 'FIV' denotes a free infectious virion – one capable of infecting a cell, integrating its genome into the host's, and transforming it into a new PIT or PIM.

The viral quasispecies existing soon after transmission is genetically homogeneous relative to later times [21,22], which at least suggests a small number of founder cells that reproduce to detectable levels. Beyond this observation, the evidence for PIM or PIT as progenitor is indirect and inconclusive at this time [23]. DCs, LCs, macrophages, and about half of the lymphocytes in normal patients express CD4, the primary receptor used by HIV to enter cells. Early viral isolates are usually M-tropic [24,25] and use the CCR5 molecule as co-receptor. LCs and macrophages express high levels of CCR5 but not CXCR4, the co-receptor for T-tropic strains that appear later in infection [26]. However, in vitro, many HIV strains, even 'T-tropic' ones, can infect Ms; 'M-tropic' strains also readily infect Ts, leading some biologists to doubt the significance of these tropisms [27]. On the PIT side, Haase et al. used in situ assays to visualize productively infected cells in recently infected lymph nodes and predominantly found T-lymphocytes, [28].

DCs and macrophages take up antigen and then migrate to lymph and spleen, [29], where they present it to T-cells. Electron micrographs show small lymphocytes locked onto larger, veiled dendritic cells like boats docked at a marina [30]. Virions can be seen budding into the spaces between the jostling cells [31]. (We have not attempted to model this interesting geometry of clustering Ms and Ts but simply assumed a well-mixed pool of cell types and virions.) A PIM arriving at the T-cell-rich paracortex of a lymph node would quickly spread the infection to Ts, which would in turn infect more Ms, and so on.

Besides possibly contributing the founder, PIMs may live longer than PITs. Investigators in the trials of highly-active antiretroviral therapy (HAART) estimated that a free virion in vivo survived for less than 6 h; a PIT, for two days; and they observed a third slope in the declining viral–load curve they interpreted as due to disappearance of productively-infected cells with a longer lifetime – which they estimated as 14–25 days [32,33]. In vitro, infected macrophages live two weeks or more, and HIV does not appear cytopathic in them [3,34]. (Migratory DCs are thought to live shorter lives, similar to that of activated T-cells [23,34].) Thus macrophages are a natural candidate for the longer-lived infected compartment.

Quiescent, infected T-cells either do not produce virions or produce at much lower levels than do activated, cycling cells [28,35,36]. By contrast, infected macrophages need not be activated to permit viral replication [37]. In vivo, about 1% of T-cells are activated at any one time [38]; this pool probably includes most PITs. Activated T-cells survive a few days in vivo; most are eliminated by programmed cell death (apoptosis) [39], although a small fraction revert to resting as 'memory' cells (see Ref. [40,41]). (For discussion of the fate of revertant, infected cells, see Section 7.) PIT lifetime might therefore simply be activated-cell lifetime; or it could be shorter due to viral cytopathicity or immune-system killing.

More recent measurements of virion lifetime in vivo – by infusing them into into monkeys – gave an even smaller figure than the HAART experiments – less than 1/2 h, [42]. To summarize the lifetime question, we assume PIMs last about two weeks; PITs, about two days; and FIVs, 20 min.

Viral production in macrophages and activated T-cells, as measured in vitro by accumulation of HIV-p24 antigen, appears similar [43,44]. Reports of virion production in PITs in vitro range from 50 to 1000 per day [45,46]; we usually took 100 as representative. Although many of these newly-budded virions will be defective or disintegrate before finding a target cell, we lump these probabilities into the infectivity parameter and simply call these virions FIVs. Both cell types exhibit a time delay in virion production: about one day in PITs [47] and four days in PIMs [43,44].

Table 1 contains our parameter choices except for virion infectivity. Although it would be interesting to estimate the latter theoretically – from the diffusion constant of a free virion, the on–off reaction rate constants with CD4 and co-receptors, the likelihood of successful genomic integration, and so on – we have not attempted it. Rather, ignoring the M-tropic vs T-tropic issue, we assumed that Ts and Ms are equally infectible; and, since the HIV protein *nef* down-regulates CD4 expression, [48], neglected co- or re-infections. Then, we adjusted the basic reproduction number R_b (see formula (5) in Section 5 or formula (A.15) in Appendix A) to yield typical growth rates, using the following calculation.

Humans have an average of 1000 $CD4^+$ T-cells per microliter in about 5 liters of peripheral blood (PB). However, 98% of lymphocytes reside in tissues; multiplying by 50 gives 2.5×10^{11} potential targets. Only 10^{-4}–10^{-3} become productively infected except in late-stage disease, yielding about 10^8 PITs. Assuming this level is attained in less than a month, with our other parameters R_b comes out in the range 5–7; we usually choose 6. For the corresponding growth curves, see Fig. 1. R_b may be considerably higher, e.g. 12, for the extremely pathogenic, 'fast' SIV strain discussed in Section 6.

This computation is also the reason we prefer 'PIT load' to viral load for normalizing growth rates. Viral load in PB varies in untreated patients over three logs, from 10^3 to 10^6 virions (or RNA-copy equivalents) per milliliter. Steady-state considerations make it clear that infected cells in PB contribute only a small (and unknown) fraction of this virus, with most due to spill-over from the enormously greater pool stored in lymph nodes.

Table 1
Parameters used for the early-infection, branching-process model

Parameter	Interpretation	Value (for rates, per day)
α	PIT production	100
β	PIM production	100
γ	PIT infectivity	(See Section 2)
η	PIM infectivity	(See Section 2)
λ	PIT progression	4.0
ζ	PIM progression	0.5
δ	V progression	72.0
sz	PIT stages	8
sm	PIM stages	8
sv	V stages	1
τz	PIT delay, stages	4
τm	PIM delay, stages	2

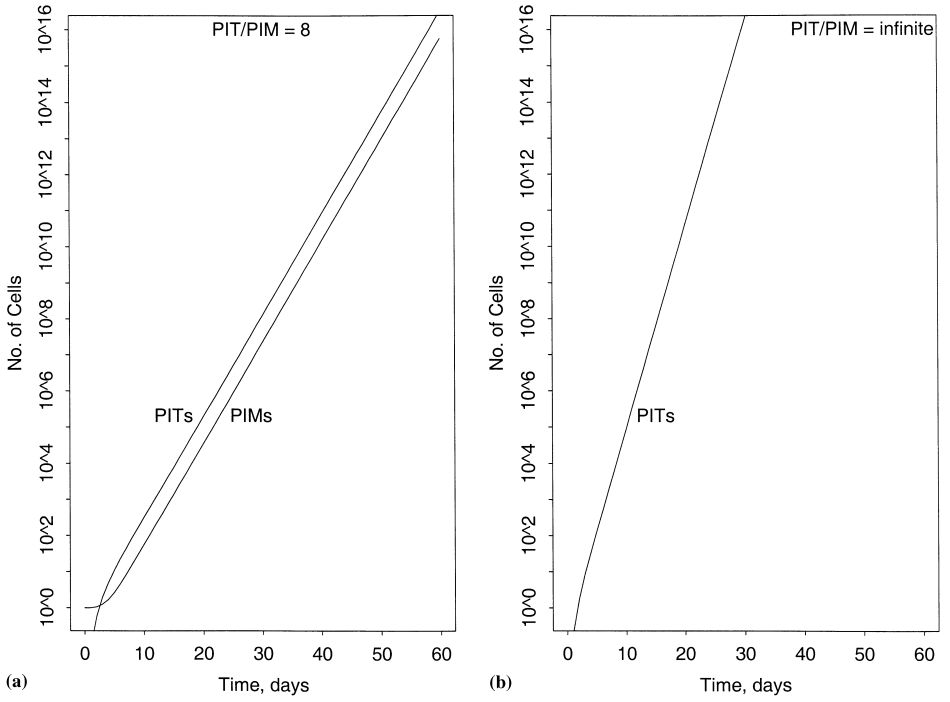

Fig. 1. Expected numbers of PITs and PIMs (left figure) or PITs (right figure) in a branching-process model of HIV or SIV infection in vivo.

In blood, lymphocytes are about eight times as frequent as monocytes, [49]. DCs and macrophages are differentiated monocytes and so presumably occur at lower frequencies. Controversy still rages over the relative contributions of PITs and PIMs to overall virion production [50–53]. Rather than resolving the controversy arbitrarily, we display results in four cases, cross-classified by cell-frequency ratio ('PIT/PIM') and founder cell (PIT or PIM). For the ratio we take the extreme cases – eight and infinity. In the former, with our parameters PITs and PIMs happen to

contribute equally; in the latter, although the founder may be a DC or LC, otherwise PIMs make a minor contribution. The reader can interpolate visually to imagine intermediate situations.

Timing cellular events such as generation times typically reveals a stochastic component, [54]. But cells are not radioactive atoms; the waiting-time distribution is usually closer to normal than to exponential, albeit with a thicker tail to the right. Accordingly, we added life-cycle 'stages', additional compartments, to the model. A gamma distribution displaces the exponential law; for five or more stages this distribution has the right shape. Setting virion production equal to zero in initial stages introduces the lags. ODE modelers already exploited this trick [55,56].

Competition among different HIV strains, especially drug-resistant strains [57], may shape the quasi-species at later times. For early infection, we make the basic assumption that viral 'daughters', whether of different or same 'mothers', neither cooperate nor compete. Since competition requires an exploited resource – for HIV in vivo it may be simply uninfected target cells – this assumption is appropriate before $CD4^+$ levels drop.

3. Informal model description

Here, we describe the branching-process model informally. For the formal implementation, see Appendix A.

To begin, let us temporarily ignore the life-stages that accommodate non-exponential waiting times and lags. Let $z(t)$, $m(t)$, and $v(t)$ be the numbers of PITs, PIMs and FIVs, respectively, existing at time t, with $t = 0$ marking the progenitor's appearance. At random times these integer-valued random variables jump up or down by one unit. Variable $v(t)$ jumps up by one whenever a FIV buds from an infected cell. The rate of jumping is proportional to the numbers of PITs and PIMs existing at that time and hence the form $\alpha z(t) + \beta m(t)$, where α and β are rate constants with units of virions per cell per day. Variables $z(t)$ and $m(t)$ jump up one unit whenever a FIV infects an uninfected cell of that type; since $v(t)$ counts only free virions, it simultaneously declines one unit. Since we are modeling early events before target-cell densities change, these rates are simply proportional to virion density and hence the form $\gamma v(t)$ and $\eta v(t)$, respectively. Finally, $z(t)$, $m(t)$, or $v(t)$, if positive, decline one unit when a cell or virion dies or loses infectiousness; the rates are of form $\lambda z(t)$, $\zeta m(t)$ and $\delta v(t)$, respectively, with λ, ζ and δ having units of inverse days.

With stages the list of random variables increases to $z_i(t)$, $m_j(t)$ and $v_k(t)$, where the indices run over the assumed number of stages. A newly-born PIT, PIM or FIV enters the first stage; it progresses to the next after an exponential waiting time with mean $[(\text{rate constant}) \cdot (\text{no. of stages})]^{-1}$; upon reaching the last stage, it dies after a similar wait. With stages, our model departs from 'pure branching', becoming of mixed, compartmental-plus-branching type. Productivity and infectivity parameters may all depend on life-stage.

The process is easily simulated on a computer. The simplest method is to generate, after each jump time, three exponential random variables with the appropriate parameters; select the smallest; increment the time by this amount; add or subtract one unit in the indicated compartment(s); and then iterate. It is essential to halt the process when the variables become so large that waiting times become infinitesimal. Although we evaluated all interesting quantities analytically or numerically, we also performed small simulation studies as a check on our programs.

4. Computing extinction probabilities

We are interested in extinction of the infection branching-process in two contexts. In one, an immune response, possibly primed by earlier vaccination, modulates some infection parameter(s); in the other, a drug changes them. For a selected parameter (e.g. virion infectiousness), either interpretation may be possible.

We consider only the simplest form of time-dependence in which a parameter changes at a selected but fixed time we call T_r (r for 'response'), which will usually be days or weeks post-exposure. (We discuss other scenarios in Section 7.) Infection may build to considerable numbers before time T_r – e.g. to millions of PITs and PIMs, see Fig. 1.

For simplicity, we omit life-cycle stages in this section. Let $I(t) \equiv z(t) + m(t) + v(t)$ be the level of infection at time t. Consider the overall infection extinction probability, QI, defined formally by

$$QI = P[I(t) = 0 \quad \text{for some } t > 0 \,|\, \text{SIC}], \tag{1}$$

where $P[\cdot|\cdot]$ denotes conditional probability of the first statement given the second and 'SIC' is short for 'standard initial conditions', which will frequently be a single PIM:

$$\text{SIC}: \quad z(0) = 0; \quad m(0) = 1; \quad v(0) = 0. \tag{2}$$

Let r, u and w denote the extinction probabilities for a process started at time T_r with one progenitor PIT, PIM, or FIV, respectively, and the post-response parameters. That is,

$$\begin{aligned} r &= P[I(t) = 0 \quad \text{for some } t > T_r \mid z(T_r) = 1;\ \text{others} = 0], \\ u &= P[I(t) = 0 \quad \text{for some } t > T_r \mid m(T_r) = 1;\ \text{others} = 0], \\ w &= P[I(t) = 0 \quad \text{for some } t > T_r \mid v(T_r) = 1;\ \text{others} = 0]. \end{aligned} \tag{3}$$

With the 'no competition or cooperation' assumption, the offspring of different 'mother' cells or virions are independent. Hence

$$QI = E[r^{z(T_r)} u^{m(T_r)} w^{v(T_r)} \,|\, \text{SIC}]. \tag{4}$$

Here '$E[\cdot|\cdot]$' is expectation with respect to the process with pre-response parameters.

Techniques to calculate QI are well known to Markov-process experts. Formula (4) states that QI equals the probability-generating function (PGF) of the process evaluated at the post-T_r extinction probabilities and at time T_r. The Kolmogorov forward equation yields a partial differential equation for the PGF which can be solved by the method of characteristics. The method yields a system of ODEs of dimension three (or, when including stages, of dimension equal to the sum-of-numbers-of-stages). The extinction probabilities defined in (3) are precisely the limit point of the ODE trajectories with the 'after response' parameters. This limit point must be a steady-state solution; hence, setting the right sides of the ODEs to zero yields equations for the desired probabilities. Some algebra reduces these equations to a one-dimensional fixed-point problem and iteration yields r, u, and w.

To compute QI, we still have to solve the ODEs with initial conditions (r, u, w) up to time T. The ODEs are non-linear and closed-form solutions are not available. However efficient computer equation-solvers can solve the system numerically. See Appendix A for the details.

5. Eradicating the infection in various scenarios

The extinction analysis yields an expression for R_b, the basic reproduction number of the process – see formula (A.15) of Appendix A – that reads, informally,

$$R_b = [\text{FIV infects PIT}] \times [\text{PIT lifetime} - \text{PIT lag}] \times [\text{PIT viral production}] + [\text{FIV infects PIM}] \times [\text{PIM lifetime} - \text{PIM lag}] \times [\text{PIM viral production}]. \quad (5)$$

The first factor in each term is the probability a virion successfully infects a cell of the corresponding type before disintegrating. Supercriticality, all extinction probabilities less than one, and $R_b > 1$ are equivalent statements.

Fig. 2 shows the effect on *QI* of lowering the virion infectivity parameter by 83.5% – changing R_b from six to just above one – at the time plotted on the abscissa. This 'intervention' could represent administration of antiretrovirals or appearance of antibodies. These graphs suggest that, if PIMs play a major role, effective therapy should begin in a week – but an additional delay of three or four days would not abolish all benefit. But if early HIV infection is primarily a T-cell disease, a delay of even two days would be ill-advised, especially if the founder is a PIT.

Of course, HAART might lower virion infectivity by 99.9%. Fig. 2 makes it clear that such high blank;efficiency is not absolutely required to have an impact on the likelihood of a chronic infection. With our model and parameters, a mere 84% represents therapeutic 'perfection', pushing *QI* all

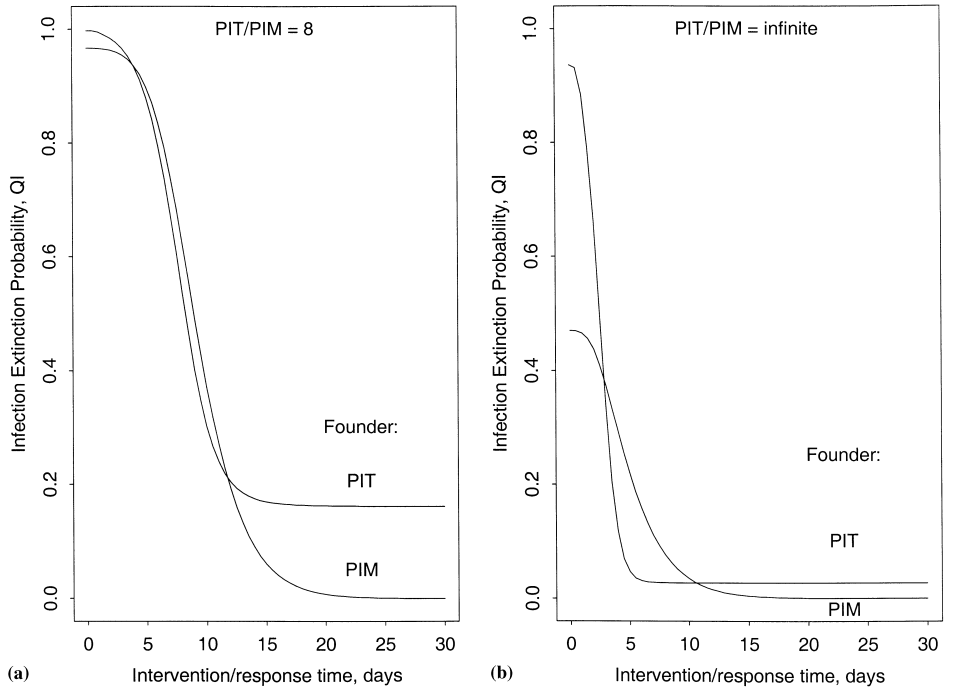

Fig. 2. Infection extinction probabilities in various scenarios explained in Section 5, plotted against time that an intervention or immune response lowers virion infectivity (drop in parameters γ and η). (a) R_b after: 1.01 (PIT/PIM = 8); (b) 1.04 (PIT/PIM = ∞).

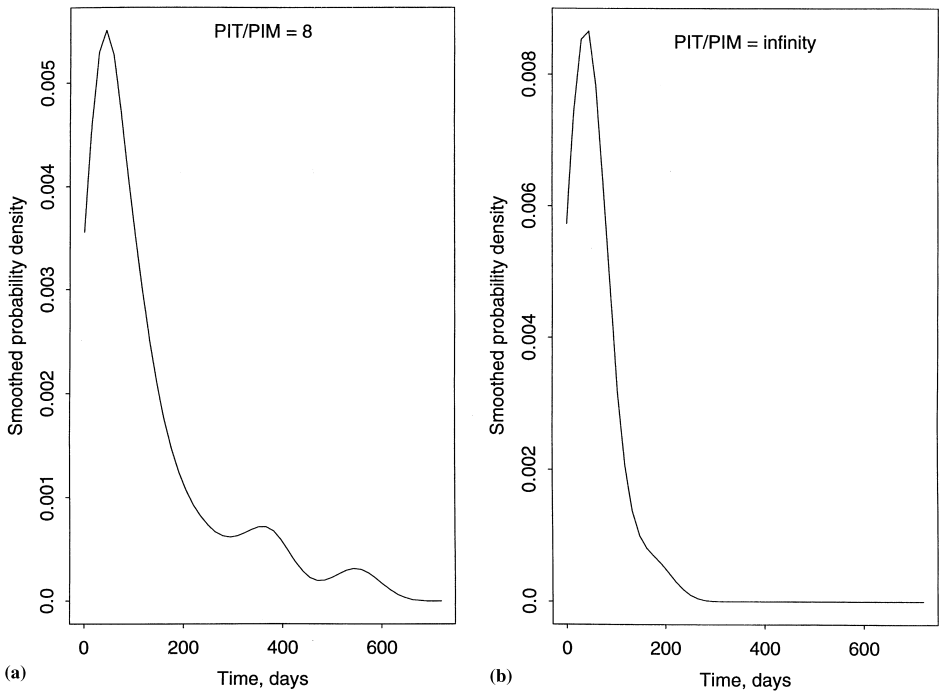

Fig. 3. Smoothed probability–density plots of extinction times in two scenarios explained in Section 5. From 200 repetitions we estimated the density at 50 points using a smoothing window of 150 days. Intervention times were: seven days on the left and three days on the right; neutrqlization was 83.5%. Cumulative probabilities (respectively, theoretical probabilities) were: 0.70 (0.701) on the left and 0.37 (0.374) on the right.

the way to one – provided the drug can be supplied for an extended period. Simulations reveal that the time-to-extinction distribution with the 'near-perfect' drug has a long tail, extending to a year or more (especially with PIT/PIM = 8); see Fig. 3. Antibodies should persist as long as antigen; taking drugs for a year should not be prohibitive. In Section 6, we compute extinction probabilities in a situation, where drugs were maintained for shorter periods.

Fig. 4 shows the effect of decreasing the PIT lifetime from two days to one 1/4 days (after-lag production lowered from one to 1/4 day), and PIM lifetime from 16 to 6 days (after-lag production drops from 12 to 2 days), at the indicated times. This 'intervention', which also lowers R_b almost to one, might reflect appearance of HIV-specific CTLs. A significant benefit accrues, especially in the mixed, PIT + PIM, scenario.

6. Application: predicting outcomes in a trial of an antiretroviral drug in monkeys

(R)-9-(2-Phosphonylmethoxypropyl)adenine (PMPA), an acyclic nucleoside phosphonate analog, is an antiretroviral compound more potent than the first to be discovered, zidovudine (AZT). In 1998, Tsai et al. [11] reported a trial of PMPA as post-exposure prophylaxis for SIV infection in macaques. The investigators inoculated 24 animals with 10 times the AID50 of a highly pathogenic SIV strain. SIV_{mne} produces very high viral loads (10^6–10^8 RNA copy

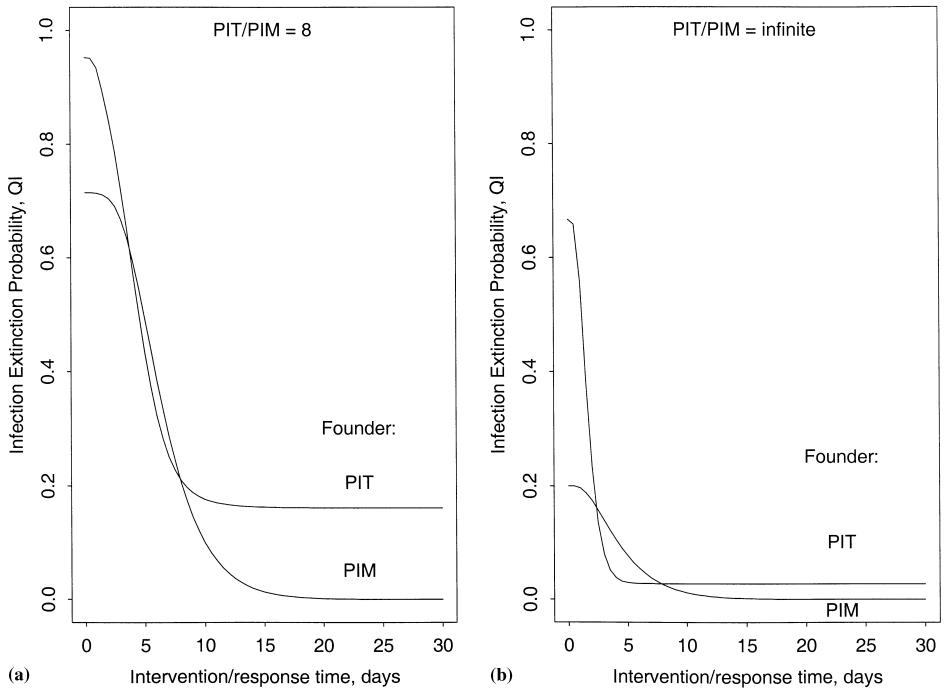

Fig. 4. Infection extinction probabilities in various scenarios explained in Section 5, plotted against time that an immune response (e.g. by HIV-specific CTLs) decreases PIT and PIM lifetimes (drop in parameters λ and ζ).

equivalents per ml) at peak viremia, which is also attained rapidly (in 2 weeks); untreated animals progress to AIDS and death in 2 years.

Tsai et al. divided the animals into six groups and, starting one, two, or three days post-inoculum, administered PMPA for three, 10, or 28 days. With 28 days treatment initiated after one day, all four animals were free of detectable virus; but some animals in the other groups suffered viral rebound. The investigators published detailed longitudinal data, with 48 weeks follow-up, including repeated measurements of viral load, percent peripheral blood mononuclear cells (PBMC) infected, and plasma antibodies. For the reader's convenience we record just the eradication vs rebound Tsai et al., data in Table 2.

In order to compare theoretical extinction probabilities with these outcomes, we first noted the whole-body 'PIT load' at peak in the control group of macaques: from 3.5×10^5 to 3.5×10^7 cells. (Calculation: 3500 PBMC/μl $\times$ 10^6 μl/l $\times$ 0.2 l $\times$ 50 LN/PB $\times$ $10^{-5} - 10^{-3}$ PIT/PBMC – Tsai et al., observed infection rate, ignoring one outlier in the untreated group. We used PIT rather than viral load to normalize, as explained in Section 2.) For any choice of R_b, the extinction probability starting with one virion, w_1, can be computed as described in Appendix A. The AID50 is then given by

$$\mathrm{AID50} = \frac{\log 2}{\log(1/w_1)} \approx \frac{0.69}{\log(1/w_1)}. \tag{6}$$

We computed the expected number of PITs at two weeks with initial condition $10 \times$ AID50 virions (by solving a linear ODE), and varied R_b, searching for a match with the selected PIT load.

Table 2
Data from Tsai et al., and theoretical infection probabilities[a]

Time p.i. (days)	Treatment period (days)			
	28	10	3	0
1	0/4 (0.09, 0.05, 0.06, 0.01)	1(1)/4 (0.70, 0.65, 0.63, 0.64)	2(1)/4 (0.83, 0.78, 0.97, 0.96)	4/4 (0.999, 0.999, 0.999, 0.999)
2	2(2)/4 (0.26, 0.13, 0.19, 0.21)			
3	2(1)/4 (0.57, 0.26, 0.46, 0.38)			

[a] Upper figures in cells are Tsai et al. data; $n(m)/N$ should be read: 'n chronic infections (and m transient infections) in N animals'. Lower 4-tuple are theoretical infection probabilities (1− extinction probabilities), for four scenarios cross-classified by PIT/PIM ratio, drug efficacy (percent reduction in virion infectivity), and expected PIT load at 14 days. The cases are, with virion dose in parentheses: 8, 99, 3.5×10^7 (128); 8, 99, 3.5×10^5 (221); ∞, 85, 3.5×10^7 (140); and ∞, 75, 3.5×10^5 (241).

Assuming daily production of 100 virions, trial-and-error gave R_b in the range 3–12. We assumed a 99% effective drug (on lowering FIV infectivity) for the mixed PIM + PIT model, and 75–85% in the PIT-alone model. Initial inoculums were in the range 128–241 virions. The higher inoculums occurred for higher peak loads and when PITs and PIMs contributed equally. Reflecting on the 'fast' SIV_{mne}, we also considered viral production per infected cell at the upper end of the reported range, 1000 per day [45,46]; this choice made no difference to extinction probabilities but increased the initial inoculum to 1315 in the PIT + PIM case.

The inoculum differences are not paradoxical. Adjusting R_b is equivalent to adjusting the infection probability of a FIV, a parameter which implicitly contains target-cell density as a factor. Given more productive capacity, matching a given load requires fewer cells, hence fewer targets, hence more virions needed in the inoculum.

Finally, we computed QI for various parameter choices and PIT loads. We display these probabilities in Table 2 for comparison to the Tsai et al. data. The patterns generated by theory and experiment are quite consistent, which is encouraging for branching-processes modeling. But the concordance should be interpreted cautiously due to the small sample size and statistical variability in the data.

Figs. 5 and 6 show the effects of varying inoculum size. Fig. 5 displays the effect of treatment delay on efficacy for a highly effective agent. We assumed PIT (14 days) $= 3.5 \times 10^7$ in both figures (the high viremia case). On the left in Fig. 5 (PIT/PIM $= 8$), R_b was 12, drug efficiency was 99%, and the inoculum was 128 virions. On the right (PIT/PIM $= \infty$), R_b was 5, drug efficiency was 85%, and the inoculum was 140 virions. (In the PIT-alone case, drug efficiency 0.99 abolished the drop in QI with time p.i. and 28 days treatment, so we display the curve for a lower efficiency.) Fig. 6 shows the interaction of efficacy, neutralization efficiency, and inoculum size for a three-day delay with 28 days treatment.

From these figures we conclude that, with high inocula and early treatment, we might underestimate a weaker agent's efficacy; but with a longer delay we risk completely dismissing a therapeutically-useful drug.

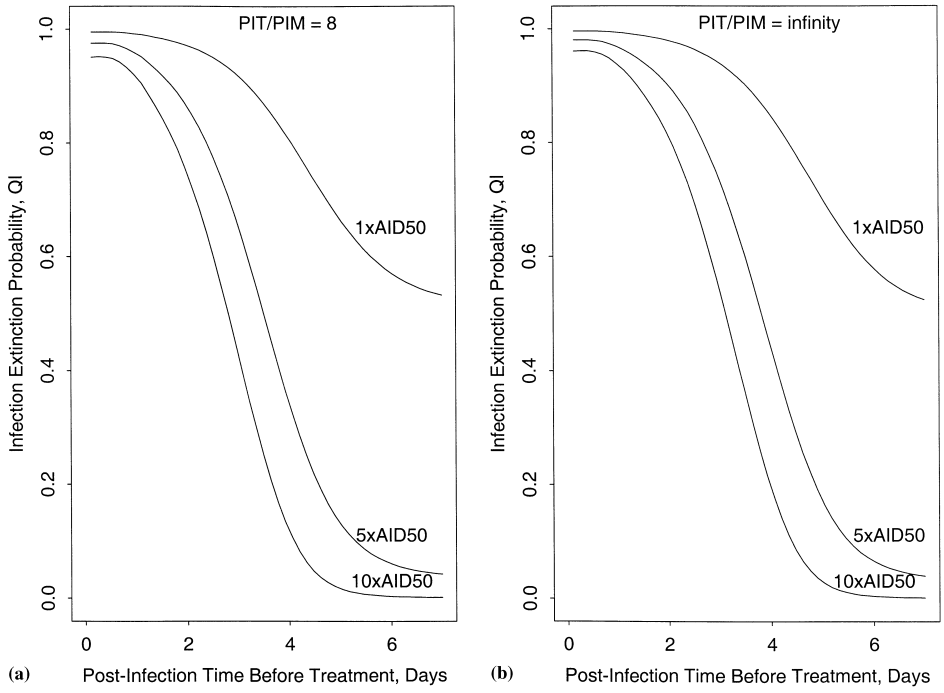

Fig. 5. Extinction probabilities for the PMPA trials as a function of time p.i., explained in Section 6.

7. Discussion

To a doctor confronted by a patient exposed to HIV through a needle-stick or unprotected sex, the important questions are: for how long must I treat, and with drugs of what potency? For a drug of moderate efficacy (e.g. 84% successful, at the cellular level, in preventing viral replication), our model suggests (see Figs. 2–4) a long treatment course of a year or more. By contrast, with a very potent but imperfect drug (e.g. 99% effective), the PMPA data and our model suggest a shorter span would suffice. Unfortunately, much uncertainty remains about the biology of primary HIV infection; only clinical trials are likely to provide definitive answers.

Consider the problem of latency. We omitted in our model a cellular pool of great importance to eradicating advanced disease, latently infected cells [58,59]. For example, activated, infected lymphocytes (our PITs) may escape death by apoptosis or immune-system killing and revert to resting. Time-to-reactivation of resting T-cells is much longer than the month or so of interest here: 70–100 days in memory cells and 500–1000 days in naïve cells [41,60], in normal patients. (With advancing disease and increasing immune activation, the rate may rise, [41,61].) Other cellular compartments, such as the central nervous system, may possess similarily long-lived, infectable cells, perhaps inaccessible to drugs.

By 'extinction' in this paper we meant extinction of the primary infection process. If other infected pools exist, true eradication might require completely suppressing viremia for an extended period. Unfortunately, we lack information about the time needed to seed these hypothetical, long-lived compartments, and their durability in the face of intervention.

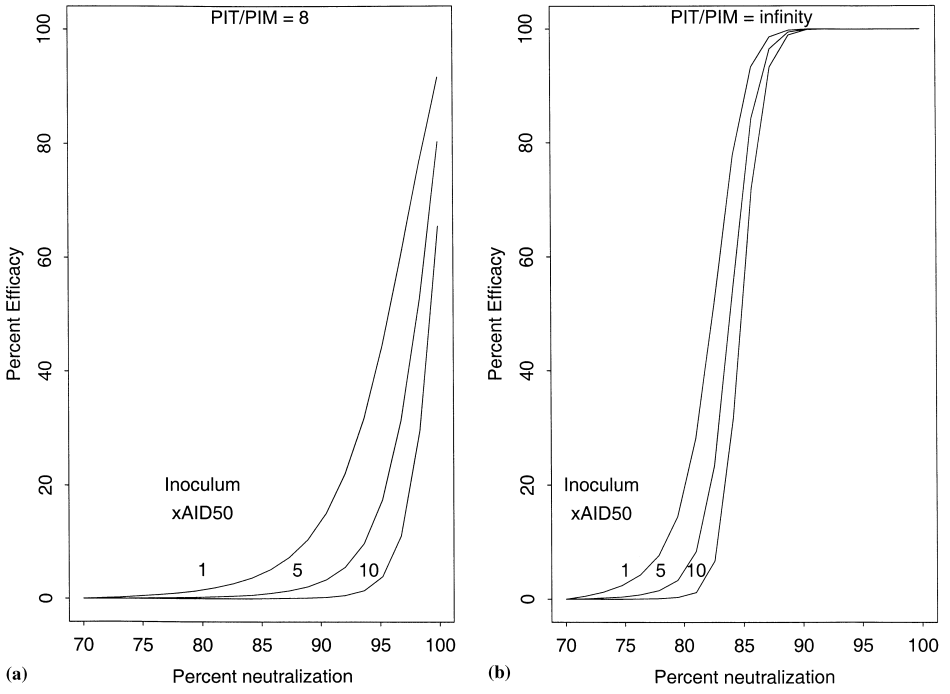

Fig. 6. Percent efficacy, defined as $100 \times \{1 - [1 - QI(\text{with drug})]/[1 - QI(\text{no drug})]\}$, plotted vs percent neutralization of virus (drop in parameters γ and η), in the PMPA trials setting explained in Section 6.

Another interesting possibility short of outright eradication is that vaccines or drugs could lower the viral set-point, perhaps delaying or even preventing progression to AIDS. Treating this scenario mathematically will require, in addition to a detailed immune-system model, a way to pass from early randomness, described by branching processes, to later deterministic dynamics, described by ODEs.

Recently, Haase and collaborators proposed that resting T-cells may be targets, may be productive when infected, and that decay of this pool better explains the third slope in the viral–load curve after HAART than macrophages [28]. SIV_{mne} (the 'fast' simian virus of Section 6) has also been shown to reproduce in non-stimulated PB cells [62]. If the reader accepts this scenario, it is only necessary to mentally replace 'PIMs' by 'RITs' –'resting, infected T-cells' – while inspecting the figures in Section 5. We will have to adjust the lifetime and productivity figures for these cells when they become better known.

Before the appearance of HIV-directed CTLs, PITs might last longer than two days. Provided PITs are activated cells, they presumably do not survive for 16 days; hence the correct extinction curve will lie between the extremes shown in the figures.

If the founder is an antigen-presenting cell (e.g. a DC), early infection might primarily involve a small subset of $CD4^+$ T-cells – those specific for HIV antigens. If so, two branching-processes occur simultaneously – the infection process modeled here, and the normal, antigen-driven expansion of $CD4^+$ cells [63]. More generally, the infection process plays out against the developing immune-system hyperactivation [40,41,64,65].

We assumed that a retroviral infection prior to an immune response can be regarded as a branching process with births, deaths, and independent descent of 'daughters'. We did not model migration of a PIM or PIT from the initial infection site to a lymph node. This possibly non-random step might occur after an initial infection burst that can be treated as a local branching-process; given transportation to lymph, extinction might be highly unlikely. Assessing the maximum delay tolerable in post-exposure prophylaxis as a function of inoculum size would help to empirically distinguish these mechanisms; a threshold would suggest the importance of transport.

In this work we treated only the simplest conception of the immune response – an instantaneous fall in virion infectivity or infected-cell lifetime. A more realistic picture will include antigen-driven branching processes of antibody-secreting B- or cell-killing T-cells. Our mathematical methods can be applied to such more-complicated models, as follows. Apoptosis or reversion to resting in activated cells terminates the immune response. Hence, we can define 'extinction' as the elimination of the last PIT, PIM and FIV and the last activated, virus-specific B- or T-cell. (This proposal runs counter to one theory of how immune-system memory is maintained – by occasional activations due to residual antigen.) We can then apply the techniques of Section 5 to compute the eradication probability. We are currently investigating detailed models of CTL and B-cell dynamics.

Acknowledgements

We thank J. McElrath, H. Mutimer, J. Overbaugh, and H. Sheppard for valuable discussions. Supported by NCI grant 1 PO1 CA76466.

Appendix A

We chose to stay in the Markov case and use the Kolmogorov equation rather than the more-popular but much-less-computationally tractable renewal equation. To allow gamma distributions and lags, we permitted any number of life-cycle stages for each compartment; we denote them by *sz*, *sm* and *sv*, respectively, and let $S = sz + sm + sv$ be the total. The state space becomes

$$X = N^{sz} \times N^{sm} \times N^{sv}, \tag{A.1}$$

where N denotes non-negative integers. Here and below, an indexed variable without an index denotes the whole n-tuple of variables e.g. $z \equiv (z_1, \ldots, z_{sz})$. So we can write $(z, m, v) \in X$.

We study a continuous-time Markov process on this countable state space. The infinitesimal generator, G, of the most general form of our process is (let f be a function of state variables)

$$\begin{aligned}[Gf](z_1, \ldots, m_1, \ldots, v_1, \ldots) = &\left(\sum_{i=1}^{sz} \alpha_i z_i + \sum_{j=1}^{sm} \beta_j m_j \right) [f(z_1, \ldots, v_1 + 1, \ldots) - f(z_1, \ldots)] \\ &+ \sum_{k=1}^{sv} \gamma_k v_k [f(z_1 + 1, \ldots, v_k - 1, \ldots) - f(z_1, \ldots)] \\ &+ \sum_{k=1}^{sv} \eta_k v_k [f(z_1, \ldots, m_1 + 1, \ldots, v_k - 1, \ldots) - f(z_1, \ldots)]\end{aligned}$$

$$
\begin{aligned}
&+ \sum_{i=1}^{sz-1} \lambda_i z_i [f(z_1, \ldots, z_i - 1, z_{i+1} + 1, \ldots) - f(z_1, \ldots)] \\
&+ \lambda_{sz} z_{sz} [f(z_1, \ldots, z_{sz} - 1, \ldots) - f(z_1, \ldots)] \\
&+ \sum_{j=1}^{sm-1} \zeta_j m_j [f(z_1, \ldots, m_j - 1, m_{j+1} + 1, \ldots) - f(z_1)] \\
&+ \zeta_{sm} m_{sm} [f(z_1, \ldots, m_{sm} - 1, \ldots) - f(z_1, \ldots)] \\
&+ \sum_{k=1}^{sv-1} \delta_k v_k [f(z_1, \ldots, v_k - 1, v_{k+1} + 1, \ldots) - f(z_1, \ldots)] \\
&+ \delta_{sv} v_{sv} [f(z_1, \ldots, v_{sv} - 1, \ldots) - f(z_1, \ldots)]. \qquad \text{(A.2)}
\end{aligned}
$$

The Greek prefactors are rates. The terms containing αs and βs represent births of virions, always into the virion first-stage, from cells in various stages; those containing γs and ηs, new infections, making first-stage PITs or PIMs and deleting a FIV; and those containing λs, ζs, or δs, progression through the stages or death.

Standard methods serve to construct the process with arbitrary initial conditions on a suitable space of (piecewise-constant, right-continuous) trajectories [66]. The Kolmogorov or forward equation reads

$$
\frac{\mathrm{d}}{\mathrm{d}t} E[f(z(t), m(t), v(t))] = E[Gf](z(t), m(t), v(t)), \qquad \text{(A.3)}
$$

where $E[\cdot]$ is the expectation with respect to the branching process with given initial conditions.

With stages, the PGF must be generalized somewhat. There are now as many arguments as stages and the PGF becomes

$$
\begin{aligned}
&\phi_t(r_1, \ldots, r_{sz}, u_1, \ldots, u_{sm}, w_1, \ldots, w_{sv}) = E(\chi_t(z_1, \ldots)), \\
&\chi_t(z_1, \ldots) \equiv \left(\prod_{i=1}^{sz} r_i^{z_i(t)} \prod_{j=1}^{sm} u_j^{m_j(t)} \prod_{k=1}^{vz} w_k^{v_k(t)} \right). \qquad \text{(A.4)}
\end{aligned}
$$

We denote the collection of variables $(r_1, \ldots r_{sz}, u_1, \ldots, u_{sm}, w_1, \ldots, w_{sv})$, which form a point in the S-dimensional unit cube, by (r, u, w), or simply by 'q'.

Below, an asterisk on an indexed quantity is a notational device whose meaning is $x_i^* = x_i$, if $i <$ the largest allowed index; $x_i^* = 1$, otherwise. Applying (A.3) to (A.4) we obtain

$$
\begin{aligned}
\frac{\mathrm{d}}{\mathrm{d}t} \phi_t(r, u, w) =& (w_1 - 1) \sum_{i=1}^{sz} E[\alpha_i z_i(t) + \sum_{j=1}^{sm} \beta_j m_j(t)] \chi_t \\
&+ \sum_{k=1}^{sv} \left(\gamma_k \left(\frac{r_1}{w_k} - 1 \right) + \eta_k \left(\frac{u_1}{w_k} - 1 \right) \right) E v_k(t) \chi_t + \sum_{i=1}^{sz} \lambda_i \left(\frac{r_{i+1}^*}{r_i} - 1 \right) E z_i(t) \chi_t \\
&+ \sum_{j=1}^{sm} \zeta_j \left(\frac{u_{j+1}^*}{u_j} - 1 \right) E m_j(t) \chi_t + \sum_{k=1}^{sv} \delta_k \left(\frac{w_{k+1}^*}{w_k} - 1 \right) E v_k(t) \chi_t. \qquad \text{(A.5)}
\end{aligned}
$$

By making the substitutions

$$Ez_i(t)\chi_t \to r_i \frac{\partial}{\partial r_i}\phi_t,$$
$$Em_j(t)\chi_t \to u_j \frac{\partial}{\partial u_j}\phi_t,$$
$$Ev_k(t)\chi_t \to w_k \frac{\partial}{\partial w_k}\phi_t$$

in (A.5), we transform it into a partial differential equation

$$\begin{aligned}\frac{\partial}{\partial t}\phi_t(r_1,\ldots) =&(w_1-1)\sum_{i=1}^{sz}\left[\alpha_i r_i\frac{\partial}{\partial r_i}+\sum_{j=1}^{sm}\beta_j u_j\frac{\partial}{\partial u_j}\right]\phi_t\\ &+\sum_{k=1}^{sv}\left[\gamma_k(r_1-w_k)+\eta_k(u_1-w_k)\right]\frac{\partial}{\partial w_k}\phi_t+\sum_{i=1}^{sz}\lambda_i\left(r^*_{i+1}-r_i\right)\frac{\partial}{\partial r_i}\phi_t\\ &+\sum_{j=1}^{sm}\zeta_j\left(u^*_{j+1}-u_j\right)\frac{\partial}{\partial u_j}\phi_t+\sum_{k=1}^{sv}\delta_k\left(w^*_{k+1}-w_k\right)\frac{\partial}{\partial w_k}\phi_t.\end{aligned} \tag{A.6}$$

We solve these equations by the method of characteristics [67]. Let $q(t)\equiv(r(t),u(t),w(t))$ be the solution of the S-dimensional system of ODEs

$$\begin{aligned}\frac{\mathrm{d}r_i}{\mathrm{d}t}&=\alpha_i(w_1-1)r_i+\lambda_i(r^*_{i+1}-r_i),\\ \frac{\mathrm{d}u_j}{\mathrm{d}t}&=\beta_j(w_1-1)u_j+\zeta_i(u^*_{j+1}-u_j),\\ \frac{\mathrm{d}w_k}{\mathrm{d}t}&=\gamma_k(r_1-w_k)+\eta_k(u_1-w_k)+\delta_k(w^*_{k+1}-w_k),\end{aligned} \tag{A.7}$$

with given initial conditions. Here the 'method of characteristics' is simply the observation that, for any $0\leqslant t\leqslant T$,

$$\frac{\mathrm{d}}{\mathrm{d}t}\phi_t(q(T-t))\equiv 0. \tag{A.8}$$

Hence

$$\phi_T(q(0))=\phi_0(q(T)). \tag{A.9}$$

As in Section 4, let $I(t)\equiv\sum z_i(t)+\sum m_j(t)+\sum v_k(t)$ be the infection level. By taking the 'after-response' extinction probabilities for each possible progenitor

$$\begin{aligned}r_i&=P[I(t)=0 \text{ for some } t>T_\mathrm{r}\mid z_i(T_\mathrm{r})=1,\ \text{others zero}],\\ u_j&=P[I(t)=0 \text{ for some } t>T_\mathrm{r}\mid m_j(T_\mathrm{r})=1,\ \text{others zero}],\\ w_k&=P[I(t)=0 \text{ for some } t>T_\mathrm{r}\mid v_k(T_\mathrm{r})=1,\ \text{others zero}]\end{aligned} \tag{A.10}$$

as initial conditions for the ODEs, we see that, provided the parameters used in the ODEs are the 'before-response' ones,

$$QI=\phi_0(r(T_\mathrm{r}),m(T_\mathrm{r}),v(T_\mathrm{r})). \tag{A.11}$$

Note that the initial conditions determine ϕ_0; e.g. for a first-stage PIM, $\phi_0(r,u,w)=u_1$.

Concerning the separate extinction probabilities defined in (A.10), for a time-homogeneous process they form the fixed point of the PGF with general initial conditions regarded as a map from the S-dimensional unit cube into itself [20]. However, rather than iterate a complicated function only available numerically on a 17-dimensional space, we relied on the fundamental formula (A.9) and some hand-algebra, as follows.

By (A.9),

$$\lim_{t\to\infty} \phi_t(r(0), u(0), w(0)) = \lim_{t\to\infty} \phi_0(r(t), u(t), w(t)). \tag{A.12}$$

If we take all components of $r(0)$, $m(0)$, and $v(0)$ less than one, the limit on the left of (A.12) exists and is the desired extinction probability. The limit on the right therefore exists and defines a limit point of the ODE trajectories, which must be a (globally-stable) steady-state solution. Markov theory also tells us that, if each state leads with positive probability to all other states, either all go extinct with probability one or all go extinct with probability less than one. Hence the stable steady-state lies inside the unit cube precisely in the supercritical case. The upshot is that setting the right sides of (A.7) equal to zero gives useful algebraic equations for the extinction probabilities.

We now restrict attention to the special case described in Section 5 – the γs, λs, ζs, and δs are stage-independent and $sz = 1$. The non-linearities in (A.7) occur only in terms containing r_1, u_1 or w_1 and we can also exploit the triangular form. Solving backwards gives

$$\begin{aligned} r_1 &= \prod_{i=1}^{sz} \frac{\lambda}{\alpha_i(1-w_1)+\lambda} \equiv F_1(w_1), \\ u_1 &= \prod_{i=1}^{sz} \frac{\zeta}{\beta_i(1-w_1)+\zeta} \equiv F_2(w_1), \\ w_1 &= \left(\frac{\gamma r_1 + \eta u_1 + \delta}{\gamma+\eta+\delta}\right) \equiv F_3(r_1, u_1). \end{aligned} \tag{A.13}$$

From (A.13), w_1 can be obtained by iterating

$$w = F_4(w) \equiv F_3(F_1(w), F_2(w)). \tag{A.14}$$

After finding w_1, we compute the other extinction probabilities by plugging back into (A.13).

Since $F_4(1) = 1$, $F_4(0) < 1$, and F_4 is monotonic, a fixed point exists in the interior of the unit interval if and only if $F_4'(1) > 1$, which yields

$$R_b \equiv \left(\frac{1}{\gamma+\eta+\delta}\right) \times \left(\frac{\gamma \sum_{i=1}^{sz} \alpha_i}{\lambda} + \frac{\eta \sum_{j=1}^{sm} \beta_j}{\zeta}\right). \tag{A.15}$$

This is the precise version of formula (5) of Section 5. Formula (A.15) also follows from the evolution equation (not shown) for the expected cell and virion counts, $Ez(t)$, $Em(t)$ and $Ev(t)$; supercriticality coincides with this linear system's $S \times S$ matrix having a positive eigenvalue. By formula (A.15) and Markov theory, the following statements are equivalent: $R_b > 1$; we are in the supercritical case; and all extinction probabilities are less than 1.

To evaluate QI using (A.11), we solved the ODE system (A.7) numerically, using a fifth-order, Runge-Kutta solver with adaptive step size and error control [68]. We also checked the iterative

solution of (A.14) against the long-time limit of the ODEs with after-treatment parameters. It is important to iterate (A.14) until the error is much smaller than the expected sizes of all compartments at time T_r. Numerical problems arise only when R_b is very close to one (where the fixed-point problem loses stability).

In Section 6, the parameters were piece-wise constant on the intervals $0 \leqslant t < T_1$, $T_1 \leqslant t < T_2$, and $T_2 \leqslant t$, where T_1 is the time post-inoculum (p.i.) and T_2 is the time p.i. plus time on treatment. To compute $\phi_{T_2}(q)$ – which, if q denotes the 'no-treatment' extinction probabilities, is the overall extinction probability – we work backwards. Let $\tilde{q}(t)$, for $T_1 \leqslant t \leqslant T_2$, solve the ODE for the parameters with treatment and with initial condition $\tilde{q}(T_1) = q$. Then $\phi_{T_2}(q) = \phi_{T_1}(\tilde{q}(T_2))$ by the argument leading to formula (A.9). So we let $\tilde{\tilde{q}}(t)$, for $0 \leqslant t \leqslant T_1$, solve the ODE for the parameters without treatment and with initial condition $\tilde{\tilde{q}}(0) = \tilde{q}(T_2)$. The argument applies again and so $\phi_0(\tilde{\tilde{q}}(T_1)$ is the desired extinction probability.

References

[1] J.O. Kahn, B.D. Walker, Acute human immunodeficiency virus type 1 infection, NEJM 339 (1) (1998) 33.
[2] M.T. Niu, D.S. Stein, S.M. Schnittman, Primary human immunodeficiency virus type 1 infection: review of pathogenesis and early treatment intervention in human and animal retroviral infections, J. Infect. Dis. 168 (1993) 1490.
[3] L.K. Schrager, M.P. D'Souza, Cellular and anatomical reservoirs of HIV-1 in patients receving potent antiretroviral combination therapy, JAMA 280 (1) (1998) 67.
[4] M.P. Busch, Time course of viremia and antibody seroconversion following human immunodeficiency virus exposure, Am. J. Med. 102 (5b) (1997) 117.
[5] J.E. Schmitz, M.J. Kuroda, S. Santra, V.G. Sasseville, M.A. Simon, M.A. Lifton, P. Racz, K. Tenner-Racz, M. Dalesandro, B.J. Scallon, J. Ghrayeb, M.A. Forman, D.C. Montefiori, E.P. Rieber, N.L. Letvin, K.A. Reimann, Control of viremia in simian immunodeficiency virus infection by $CD8^+$ lymphocytes, Science 283 (1999) 857.
[6] X. Jin, D.E. Bauer, S.E. Tuttleton, S. Lewin, A. Gettie, J. Blanchard, C.E. Irwin, J.T. Safrit, J. Mittler, L. Weinberger, L.G. Kostrikis, L. Zhang, A.S. Perelson, D.D. Ho, Dramatic rise in plasma viremia after CD8(+) T-cell depletion in simian immunodeficiency virus-infected macaques, J. Exp. Med. Mar 15. 189 (6) (1999) 991.
[7] A.N. Phillips, Reduction of HIV concentration during acute infection: independence from a specific immune response, Science 271 (1996) 497.
[8] R.J. De Boer, A.S. Perelson, Target-cell limited and immune control models of HIV infection: a comparison, J. Theor. Biol. 190 (3) (1998) 201.
[9] V. DeGrutolla, G.H. Seage, K.H. Mayer, C.R. Horsburgh Jr., Infectiousness of HIV between male homosexual partners, J. Clin. Med. 42 (1989) 849.
[10] N.P. Jewel, S. Siboski, Statistical analysis of HIV infectivity based on partner studies, Biometrics 46 (1990) 1133.
[11] C.-C. Tsai, P. Emau, K.E. Follis, T.W. Beck, R.E. Beneveniste, N. Bischofberger, J.D. Lifson, W.R. Morton, Effectiveness of post-inoculation (R)-9-(2-Phosphonylmethoxypropyl) adenine treatment for prevention of persistent simian immunodeficiency virus SIV_{mne} infection depends critically on timing of initiation and duration of treatment, J. Virol. 72 (1998) 4265.
[12] T. Hraba, J. Dolezal, Mathematical model of $CD4^+$ lymphocyte depletion in HIV infection, Folia Biol (Praha) 35 (3) (1989) 156.
[13] M.A. Nowak, R.M. May, Mathematical biology of HIV infections: antigenic variation and diversity threshold, Math. Biosci. 106 (1991) 1.
[14] M.A. Nowak, A.L. Lloyd, G.M. Vasquez et al., Viral dynamics of primary viremia and antiretroviral therapy in simian immunodeficiency virus infection, J. Virol. 71 (1997) 7518.
[15] M. Turelli, Random environments and stochastic calculus, Theor. Popul. Biol. 12 (1977) 140.

[16] P. Jagers, Branching Processes with Biological Applications, Wiley, New York, 1975.
[17] S. Moolgavkar, D. Venzon, Two-event model for carcinogenesis: incidence curves for childhood and adult tumors, Math. Biosci. 47 (1979) 55.
[18] S. Moolgavkar, G. Luebeck, Two-event model for carcinogenesis: biological, mathematical, and statistical considerations, Risk Anal. 10 (2) (1990) 323.
[19] R.M. Anderson, R.M. May, Infectious diseases of humans: dynamics and control, Oxford University, Oxford, 1991.
[20] C.J. Mode, Multitype Branching Processes: Theory and Applications, Elsevier, Amsterdam, 1971.
[21] T. Zhu, H. Mo, N. Wang, Y. Cao, R.A. Koup, D.D. Ho, Genotypic and phenotypic characterization of human immunodeficiency virus type 1 in patients with primary infection, Science 261 (1993) 1179.
[22] T. Zhu, N. Wang, A. Carr, D.S. Nam, R. Moor-Jankowski, D.A. Cooper, D.D. Ho, Genetic characterization of human immunodeficiency virus type 1 in blood and genital secretions: evidence for viral compartmentalization during sexual transmission, J. Virol. 70 (5) (1996) 3098.
[23] A. Blauvelt, The role of skin dendritic cells in the initiation of human immunodeficiency virus infection, Am. J. Med. 102 (5B) (1997) 16.
[24] H.M. Schuitemaker, H.M. Koot, N.A. Kootstra, M.W. Dercksen, R.E. Goede, R.P. van Steenwijk, J.M. Lange, J.K. Schattenkerk, F. Miedema, M. Tersmette, Biological phenotype of human immunodeficiency virus type 1 clones at different stages of infection: progression of disease is associated with a shift from monocytotropic to T-cell-tropic virus populations, J. Virol. 66 (1992) 1354.
[25] van't Wout, A.B.N.A. Kootsra, G.A. Mulder-Kampinga, N. Albrecht-van Lent, H.J. Scherpier, J. Veenstra, K. Boer, R.A. Coutinho, F. Miedema, H. Schuitemaker, Macrophage-tropic variants initiate human immunodeficiency virus type 1 infection after sexual parenteral and vertical transmission, J. Clin. Invest. 94 (1994) 2060.
[26] M. Zaitseva, A. Blauvelt, S. Lee, C.K. Lapham, V. Klaus-Kovtun, H. Mostowki, J. Manischewitz, H. Golding, Expression and function of CCR5 and CXCR4 on human Langerhans cells and macrophages: implications for primary HIV infection, Nat. Med. 3 (1997) 1369.
[27] G. Stent, G.B. Joo, P. Kierulf, B. Asjo, Macrophage tropism: fact or fiction? J. Leukoc. Biol. Jul. 62 (1) (1997) 4.
[28] A. Haase, presentation at Fred Hutchinson CRC, Seattle, June 1999.
[29] R. van Furth, H. Beekhoizen, Monocytes, in: Encyclopedia of Immunology, 2nd Ed., Academic Press, New York, 1998.
[30] J. Atzpodien, K.E.J. Dittmar, Images in clinical medicine, New Eng. J. Med. 340 (1999) 1732.
[31] J. McElrath, Seminar presentation, March 1999, University of Washington, Seattle.
[32] A.S. Perelson, P. Essunger, C. Yunzhen, M. Vesanen, A. Hurley, K. Saksela, M. Markowitz, D.D. Ho, Decay characteristics of HIV-1 infected compartments during combination therapy, Nature 387 (1997) 188.
[33] V. Finzi, M.H. Hermanlova, T. Pierson et al., Identification of a reservoir for HIV-1 patients on highly active antiretroviral therapy, Science 278 (1997) 1295.
[34] R. van Furth, Origin and turnover of monocytes and macrophages, Curr. Top. Pathol. 79 (1989) 125.
[35] J.A. Zack, A.J. Cann, J.P. Lugo, I.S.Y. Chen, AIDS virus production from infected peripheral blood T-cells following HTLV-1 induced mitogenic stimulation, Science 240 (1988) 1026.
[36] D. Zagury, J. Bernard, R. Leonard, R. Cheynier, M. Feldman, P.S. Sarin, R.C. Gallo, Long-term cultures of HTLV-III infected cells: a model of cytopathology of T-cell depletion in AIDS, Science 231 (1986) 850.
[37] M. Stevenson, H.E. Gendelman, Cellular and viral determinants that regulate HIV-1 infection in macrophages, J. Leukoc. Biol. 56 (1994) 278.
[38] N. Sachsenberg, A.S. Perelson, S. Yerly, G.A. Schockmel, D. Leduc, B. Hirschel, L. Perrin, Turnover of $CD4^+$ and $CD8^+$ T-lymphocytes in HIV-1 infection as measured by Ki-67 antigen, J. Exp. Med. 187 (8) (1998) 1295.
[39] E.S. Razvi, R.R. Welsh, Apoptosis in viral infections, in: Advances in Viral Research, vol. 45, Academic Press, New York, 1995.
[40] D. Wick, The disappearing $CD4^+$ T-cells in HIV infection: a case of over-stimulation? J. Theor. Biol. 197 (1999) 507.
[41] D. Wick, On T-cell dynamics and the hyperactivation theory of AIDS pathogenesis, Math. Biosci. 158 (1999) 127.
[42] T. Igarashi, C. Brown, A. Azadegan, N. Haigwood, D. Dimitrov, M.A. Martin, R. Shibata, Human immunodeficiency virus type 1 neutralizing antibodies accelerate clearance of cell-free virions from blood plasma, Nat. Med. 5 (2) (1999) 211.

[43] J.B. Weinberg, T.J. Matthews, B.R. Cullen, Productive HIV-1 infection of non-proliferating human monocytes, J. Exp. Med. 174 (1991) 1477.
[44] W.P. Tsai, S.R. Conley, H.F. Kung, R.R. Garrity, P.L. Nara, Preliminary in vitro growth cycle and transmission studies of HIV-1 in an autologous primary cell assay of blood-derived macrophages and peripheral blood mononuclear cells, Virology 226 (2) (1996) 205.
[45] D.S. Dimitrov, R.L. Wiley, H. Sato, L.J. Chang, R. Blumenthal, M.A. Martin, Quantitation of human immunodeficiency virus type 1 infection kinetics, J. Virol. 67 (1993) 2182.
[46] S. Kim, R. Byrn, J. Goopman, D. Baltimore, Temporal aspects of DNA and RNA synthesis during human immunodeficiency virus infection: evidence for differential gene expression, J. Virol. 63 (9) (1989) 3708.
[47] M.G. Pellegrino, G. Li, M.J. Potash, D.J. Volsky, Contribution of multiple rounds of viral entry and reverse transcription of expression to human immunodeficiency virus type 1, J. Biol. Chem. 266 (1991) 1783.
[48] C. Aiken, J. Konner, N.R. Landau, M.E. Lenburg, D. Trono, Nef induces CD4 endocytosis: requirement for a critical dileucine motif in the membrane-proximal CD4 cytoplasmic domain, Cell 76 (5) (1994) 853.
[49] J.H. Jandl (Ed.), Blood: Textbook of Hematology, Little Brown, New York, 1996, p. 54.
[50] D. Mcllroy, B. Autran, R. Cheynier, J.P. Clauvel, E. Oksenhendler, P. Debre, A. Hosmalin, Low infection frequencies of macrophages in the spleens of HIV-1 + patients, Res. Virol. 147 (2&3) (1996) 115.
[51] M.J. McElrath, J.E. Pruett, Z.A. Cohn, Mononuclear phagocytes of blood and bone marrow: comparative roles as viral reservoirs in human immunodeficiency virus type 1 infections, Proc. Nat. Acad. Sci. USA 86 (2) (1989) 675.
[52] J.M. Orenstein, C. Fox, S.M. Wahl, Macrophages as a source of HIV during opportunistic infections, Science 276 (1997) 1857.
[53] H. Mutimer, PhD thesis, Monash University, 1998.
[54] J.L. Lebowitz, S.I. Rubinow, A theory for the age and generation time distribution of a microbial population, J. Math. Biol. 1 (1974) 17.
[55] Z. Grossman, M. Feinberg, V. Kuznetsov, D. Dimitrov, W. Paul, HIV infection: how effective is drug combination treatment? Immunol. Today 19 (11) (1998) 528.
[56] J.E. Mittler, B. Sulzer, A.U. Neumann, A.S. Perelson, Influence of delayed viral production on viral dynamics in HIV-1 infected patients, Math. Biosci. 152 (1998) 143.
[57] A. McLean, M.A. Nowak, Comptition between zidovudine-sensitive and zidovudine-resistant strains of HIV, AIDS 6 (1) (1992) 71.
[58] T.W. Chun, D. Engel, M.M. Berrey, T. Shea, L. Corey, A.S. Fauci, Early establishment of a pool of latently infected, resting $CD4^+$ T-cells during primary human immunodeficiency virus 1 infection, Proc. Nat. Acad. Sci. USA 95 (1998) 8869.
[59] D. Finzi, J. Blankson, J.D. Siliciano, J.B. Margolick, K. Chadwick, T. Pierson, K. Smith, J. Lisziewicz, F. Lori, S. Gamne, J. Gallant, R.F. Siliciano, Latent infection of $CD4^+$ T-cells provides a mechanism for lifelong persistence of human immunodeficiency virus 1 even in patients on effective combination therapy, Nat. Med. 5 (5) (1999) 512.
[60] A. McLean, A.C. Michie, In vivo estimates of division and death rates of human T-lymphocytes, Proc. Nat. Acad. Sci. USA 92 (1995) 3707.
[61] D. Wick, Tap-and-drain versus general activation: steady-states and the AIDS paradox, preprint, 1999.
[62] J.T. Kamata, A. Mozaffarian, J. Overbaugh, J. Virol. 72 (1) (1998) 245.
[63] Zvi Grossman, M. Polis, M.B. Feinberg, Zehava Grossman, I. Levi, S. Jankelevich, R. Yarchoan, J. Boon, F. de Wolf, J.M.A. Lange, J. Goudsmit, D.S. Dimitrov, W.E. Paul, Attenuated decline of HIV infection under HAART, preprint, May 1999.
[64] M.S. Ascher, H.W. Sheppard, AIDS as immune system activation: a model for pathogenesis, Clin. Exp. Immunol. 73 (1988) 165.
[65] G. Pantaleo, A.S. Fauci, HIV-1 infection in the lymphoid organs: a model for disease development, J. NIH Res. 5 (1993) 68.
[66] D. Freedman, Approximating Countable Markov Chains, Holden-Day, San Francisco, 1971.
[67] F. John, Partial Differential Equations, Springer, New York, 1971.
[68] W.H. Press, B.P. Flannery, S.A. Teukolsky, W.T. Vetterling, Numerical Recipes in C, section 15.2, Cambridge University, Cambridge, 1988.